Hyperfine Interact
DOI 10.1007/s10751-012-0722-4

Mössbauer spectra of iron-doped titanium dioxide fine particles prepared by a soft chemical solution method

Junhu Wang · Yoichi Sakai

Abstract Chemical states of iron species were investigated in Fe-doped titanium dioxide (TiO_2) by means of ^{57}Fe-Mössbauer spectroscopy. Fe-doped samples, $Ti_{1-x}Fe_xO_2$ where x ranged from 0.01 to 0.1, were prepared by a soft chemical solution method. As for the samples heated at 500 °C in air as the final process of preparation, iron species at $x = 0.01$ was assigned to high-spin Fe^{3+} tetrahedrally coordinated with four oxide anions, while ones at $x = 0.1$ to high-spin Fe^{3+} octahedrally coordinated with six oxide anions.

Keywords ^{57}Fe-Mössbauer spectroscopy · Iron-doped titanium dioxide · Soft chemical solution method · Tetrahedral sites · Octahedral sites

1 Introduction

There have been a number of researches on titanium dioxide (TiO_2), where the photocatalytic activities are noted especially [1]. It was reported that doping of a small amount of iron to TiO_2 enhanced the catalytic activity. It is expected that Fe ions in TiO_2 should affect the photo-redox-reactions [2–4]. In this work, ferric ions were doped in TiO_2 and the physical and chemical states of doped Fe were investigated by ^{57}Fe-Mössbauer spectroscopy in order to gain clues for the chemical roles of iron ions in photocatalytic reactions.

J. Wang
Dalian Institute of Chemical Physics, Chinese Academy of Science, Dalian 116023, China

Y. Sakai (✉)
Daido University, Nagoya 457–8530, Japan
e-mail: yocsakai@daido-it.ac.jp

2 Experimental

2.1 Materials

Chemical reagents used were commercially available. According to a soft chemical solution method similar to our previous work [5], Fe-doped TiO_2 samples were prepared as follows; a 2-ethoxy-ethanol solution of titanium(IV) iso-propylate and a 2-ethoxy-ethanol solution of iron(III) acetylacetonate were mixed with a various ratio ($x = 0.01$, 0.025, 0.05, 0.1 for $Ti_{1-x}Fe_xO_2$). The mixture solution was heated, after adding aqueous hydrogen peroxide (35 %). The product obtained by evaporating-up of the solution was dried in air. Some portions of the resultant powder were submitted to a powder XRD and ^{57}Fe-Mössbauer measurements. The others were additionally calcined at 500 °C for 2 h before the measurements.

2.2 Powder XRD measurements

The XRD patterns for the $Ti_{1-x}Fe_xO_2$ samples were measured at room temperature by a conventional way using a RIGAKU MiniFlex diffractometer with Cu Kα radiation ($\lambda = 0.154$ nm).

2.3 ^{57}Fe-Mössbauer measurements

Mössbauer measurements were performed in an ordinary mode with Mössbauer spectrometers, fabricated by Toporogic Systems Inc., with a ^{57}Co(Rh) source. Measurement temperature was ranged from 78 K to 300 K regulated by a liquid-N_2 cryostat of Oxford DN1726. The spectral curve fitting was carried out by using a Mössbauer analysis program, MossWinn 4.0Pre. The isomer shift (IS) and Doppler velocity scale were calibrated with respect to metallic iron at room temperature.

3 Results and discussion

Powder XRD patterns of $Ti_{1-x}Fe_xO_2$ are shown in Fig. 1; the left ones are for the samples as chemically-prepared without calcining, and the right ones for the samples after calcining at 500 °C for 2 h.

The XRD patterns for the samples not calcined show that there were observed both the rutile and anatase phase at $x = 0$, i.e., without iron-doping, while the anatase peak intensities were enhanced with almost-vanishing of rutile phase for the iron-doped TiO_2 samples. The representative peaks for rutile and anatase phases are seen at $2\theta = 27.6°$ and $25.6°$, respectively. As for the samples calcined at 500 °C, it was revealed that the $Ti_{1-x}Fe_xO_2$ samples at $x = 0.01$, 0.025, 0.05 and 0.1 were in in anatase/rutile nano-composite phases, while pure TiO_2, that is, $x = 0$, had only rutile phase. It is obvious that the anatase phase should be formed by incorporation of ferric cations into TiO_2.

In the figure, we can apparently recognize line-broadening due to small-size crystallite effect, from which the average particle sizes were roughly estimated by applying the Scherer equation in the followings; for the non-heated samples, the particle size was 19 nm in rutile at $x = 0$, the size of anatase was ranged from 20 to 3 nm at

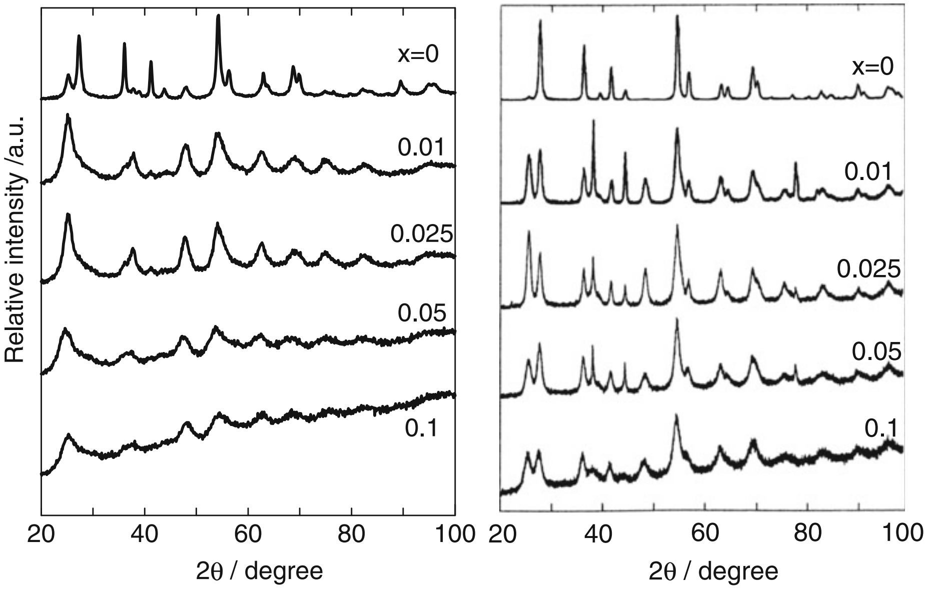

Fig. 1 XRD patterns of $Ti_{1-x}Fe_xO_2$. the left ones; the samples as prepared (without calcining). the right ones; the samples after calcining at 500 °C for 2 h

$x = 0$ to 0.1, respectively. As for the calcined samples, the average particle size was 28 to 4 nm ($x = 0$ to 0.1) for rutile, and 8 to 4 nm ($x = 0.01$ to 0.1) for anatase.

In Fig. 2, Mössbauer spectra at 298 K and 78 K of Fe-doped $Ti_{1-x}Fe_xO_2$ are shown, where x is an atomic substitution fraction of iron; the left ones are for the samples as chemically-prepared without calcining, and the right ones for the samples after calcining at 500 °C for 2 h. The dotted lines are just for eye-guide to help to identify an absorption peak position at a glance.

It was revealed that the iron states should be high-spin type ferric ion Fe^{3+} octahedrally coordinated with six oxide anions from the isomer shift values of 0.32 to 0.40 mm/s. As seen in the right part of Fig. 2 for the samples heated at 500 °C, both the spectral absorptions with $x = 0.01$ and 0.1 consist of one doublet at 298 K, whose IS values were evaluated to be 0.22 and 0.34 mm/s for those at $x = 0.01$ and 0.1, respectively, by our curve-fitting. The two IS values should be both assigned to high-spin type ferric ion (Fe^{3+}); the former to Fe^{3+} tetrahedrally coordinated with four oxide ions (O^{2-}), while the latter to Fe^{3+} octahedrally with six O^{2-} ions [6]. The spectra at 298 K and 78 K of $Ti_{0.90}Fe_{0.10}O_2$ in the Fig. 2 showed no magnetic sextet absorption, revealing that there was not found hematite (α-Fe_2O_3) which had been reported to exist in $Ti_{0.90}Fe_{0.10}O_2$ and $Ti_{0.85}Fe_{0.15}O_2$ by Zhu et al. [2], who prepared their samples by a sol-gel doping method. It is likely implied from no observation of such a sextet even at 78 K that fine-particles of hematite, in superparamagnetic states, should not be formed in our iron-doping procedure. This was also supported by the present XRD data in Fig. 1, showing no peak ascribable to hematite.

Both the room-temperature spectra at $x = 0.025$ and 0.05 could be decomposed into the two doublets observed for $x = 0.01$ and 0.1, revealing that there were coexisting tetrahedral $Fe^{3+}O_4^{2-}$ and octahedral $Fe^{3+}O_6^{2-}$ species. The relative area

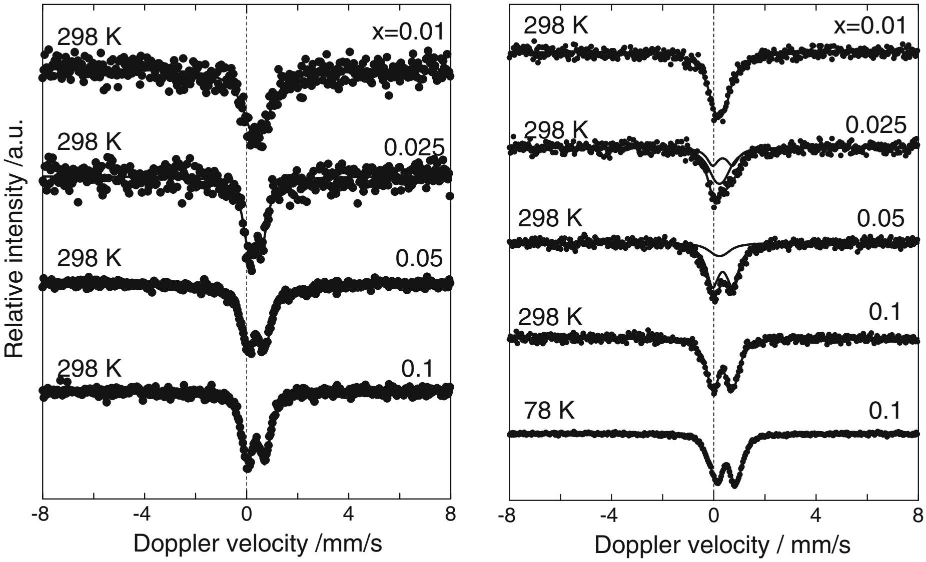

Fig. 2 Mössbauer spectra at 298 K and 78 K of $Ti_{1-x}Fe_xO_2$ ($x = 0.01$, 0.025, 0.05, and 0.1). The *dotted lines* are just for eye-guide. the left-handed one; the samples as prepared (without calcining). the right-handed one; the samples after calcining at 500 °C for 2 h

Fig. 3 Iron-substitution-fraction (x)-dependences of relative Mössbauer spectral area; circle; Fe^{3+} species with a lower IS value, square; Fe^{3+} species with a higher IS value

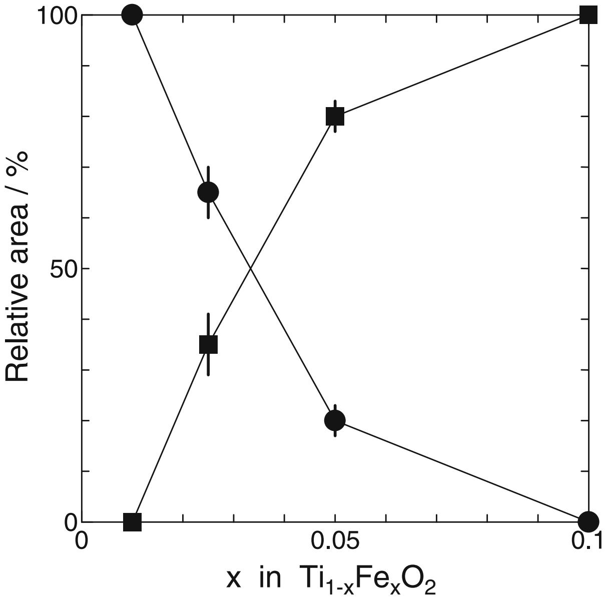

intensities of the $Fe^{3+}O_4^{2-}$ and $Fe^{3+}O_6^{2-}$ species, with a lower IS and a higher IS, respectively, are plotted against the iron fraction x in Fig. 3. It is assumed that Fe^{3+}doping into TiO_2 should occur at first predominantly at tetrahedral sites. After

Fig. 4 Temperature-dependent Mössbauer-absorption area of $Ti_{0.99}Fe_{0.01}O_2$ and $Ti_{0.90}Fe_{0.10}O_2$. In the ordinate scale, A and A_{78} are absorption areas at T and 78 K, respectively

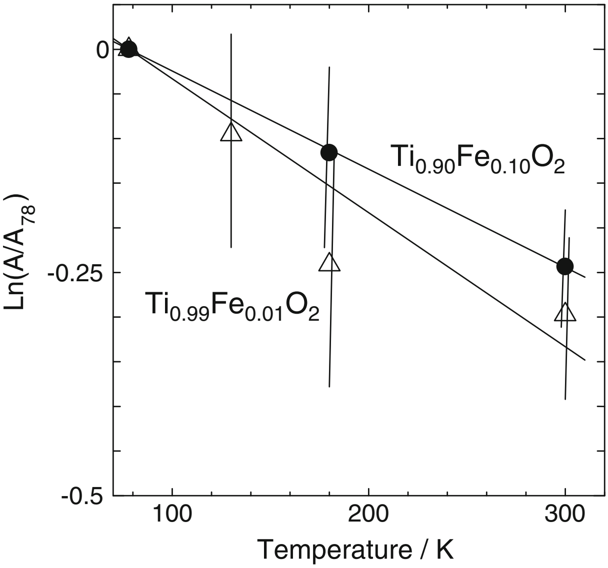

completing the iron-doping at the tetrahedral sites to a relatively small extent, the replacement of octahedral Ti^{4+} ions with Fe^{3+} ions start.

As to doped ferric ion's sites in TiO_2, Nishida et al. proved in 1990s that Fe^{3+} ions preferred to occupy the tetrahedral sites surrounded by four O^{2-} ions rather than the octahedral sites; in the Mössbauer spectrum at room temperature of their $45K_2O{\cdot}50TiO_2{\cdot}5Fe_2O_3$ glass sample, only a tetrahedral-site Fe^{3+} component appeared, although both tetrahedral and octahedral sites were confirmed to exist by the infra-red spectroscopy of the same sample [7, 8].

In order to confirm our assignment above, the temperature dependences of Mössbauer absorption area of $Ti_{0.99}Fe_{0.01}O_2$ and $Ti_{0.90}Fe_{0.10}O_2$ were investigated. The results are shown in Fig. 4, where the natural logarithm of the ratio A/A_{78} (A and A_{78}, absorption areas at T and 78 K, respectively) is plotted against temperature T. According to Matsubara et al. [9], the slope (k) of such a plot is proved to be related to force constant (α) in the following expression; $k = -1/\alpha$. As shown in Fig. 4, the value of α is observed to be larger in $Ti_{0.90}Fe_{0.10}O_2$ than $Ti_{0.99}Fe_{0.01}O_2$, implying that the doped ferric ions should be incorporated more rigidly in $Ti_{0.90}Fe_{0.10}O_2$. Therefore, it might be valid to our assignment that the 1 %-doped ferric ions might occupy at the tetrahedral sites while the 10 %-ones at the octahedral sites, since the more rigidly Mössbauer atoms in crystal lattice sites could be restricted, the higher coordination number the atoms have.

4 Conclusion

It was revealed from our powder XRD measurements that iron-doping to TiO_2 should lead to the anatase structure as a dominant crystalline phase, while the rutile phase be to a much greater extent without iron-doping. In the present Mössbauer spectra, there were mainly found ferric ions Fe^{3+} octahedrally coordinated with six oxide anions. However, for the Fe-doped TiO_2 samples with a small iron-content after calcining at 500 °C, ferric ions were observed to exist in a tetrahedral arrangement surrounded by four O^{2-} anions. In our doping-procedure, there was formed no aggregated particle of hematite showing weak-ferromagnetism or super-paramagnetism.

References

1. Ollis, D., et al.: Appl. Catal., B Environ. **99**, 377 (2010)
2. Zhu, S., et al.: Hyperfine Interact. **165**, 273 (2005)
3. Bajoczi, E.G., et al.: Appl. Catal., B Environ. **103**, 232 (2011)
4. Vejpravona, J.P., et al.: Intern. J. Chem. Biol. Eng. **6**, 34 (2012)
5. Wang, J., et al.: Chem. Mater. **18**, 2261 (2006)
6. Menil, F.: J. Phys. Chem. Solids **46**, 763 (1985)
7. Nishida, T.: Mössbauer effect in inorganic glasses. In: Vertes, A., Homonnay, Z. (eds.) Mössbauer Spectroscopy of Sophisticated Oxides, chapter 2, pp. 27–87. Akademiai Kiado, Budapest (1996)
8. Nishida, T., et al.: Bull. Chem. Soc. Jpn. **64**, 154 (1991)
9. Matsubara, S., et al.: J. Phys. **40**, C2, 363 (1979)